

**THE CRYSTAL STRUCTURE OF DELINDEITE,  
Ba<sub>2</sub>{(Na,K,□)<sub>3</sub>(Ti,Fe)[Ti<sub>2</sub>(O,OH)<sub>4</sub>Si<sub>4</sub>O<sub>14</sub>](H<sub>2</sub>O,OH)<sub>2</sub>}, A MEMBER  
OF THE MERO-PLESIOTYPE BAFERTISITE SERIES**

GIOVANNI FERRARIS<sup>§</sup> AND GABRIELLA IVALDI

*Dipartimento di Scienze Mineralogiche e Petrologiche, Università di Torino, Via Valperga Caluso 35, I-10125 Torino, Italy*

DMITRY YU. PUSHCHAROVSKY, NATALIA V. ZUBKOVA AND IGOR V. PEKOV

*Department of Geology, Moscow State University, 119899 Moscow, Russia*

ABSTRACT

By using a crystal from a new locality, the structure of delindeite has been refined to  $R = 0.054$  for 703 unique reflections with  $I > 2\sigma(I)$ . This titanosilicate [ideally Ba<sub>2</sub>{(Na,K,□)<sub>3</sub>(Ti,Fe)[Ti<sub>2</sub>(O,OH)<sub>4</sub>Si<sub>4</sub>O<sub>14</sub>](H<sub>2</sub>O,OH)<sub>2</sub>}, space group  $A2/m$ ,  $a$  5.327(2),  $b$  6.856(2),  $c$  21.51(3) Å,  $\beta$  93.80(4)°,  $Z = 2$ ,  $D_{\text{calc.}} = 3.815$  g/cm<sup>3</sup>, belongs to a large group of bafertisite-like structures characterized by an ideally octahedral (*O*) sheet sandwiched between two heteropolyhedral (*H*) sheets; these sheets are formed by Ti-octahedra and disilicate groups [Si<sub>2</sub>O<sub>7</sub>]. The *O* sheet in delindeite comprises a large (Na,K) polyhedron together with octahedral Na and Ti sites; the alkali polyhedra are partially vacant. The large Ba cation is localized in the interlayer. Evidence of the leaching of alkalis, related atomic disorder, and the position of delindeite within the bafertisite polysomatic series are discussed. On the whole, this series is considered of mero-plesiotype. In fact, the heterophyllosilicate *HOH* layer, to a first approximation, represents the common module in this series, whereas the interlayer content is variable (merotypism), and may modify its structure in different members (plesiotypism).

*Keywords:* delindeite, crystal structure, polysomatic bafertisite series, titanosilicates, heterophyllosilicates, merotypism, plesiotypism.

SOMMAIRE

En utilisant un cristal d'une localité nouvelle, nous avons réussi à affiner la structure de la delindéite jusqu'à un résidu  $R$  de 0.054 pour 703 réflexions uniques dont l'intensité dépasse  $2\sigma$ . Ce titanosilicate, dont la composition idéale serait Ba<sub>2</sub>{(Na,K,□)<sub>3</sub>(Ti,Fe)[Ti<sub>2</sub>(O,OH)<sub>4</sub>Si<sub>4</sub>O<sub>14</sub>](H<sub>2</sub>O,OH)<sub>2</sub>}, groupe spatial  $A2/m$ ,  $a$  5.327(2),  $b$  6.856(2),  $c$  21.51(3) Å,  $\beta$  93.80(4)°,  $Z = 2$ ,  $D_{\text{calc.}} = 3.815$  g/cm<sup>3</sup>, fait partie d'un groupe important de structures ressemblant à celle de la bafertisite, et contenant un feuillet *O* d'octaèdres (idéalement) entre deux feuillets *H* hétéropolyédriques; ceux-ci contiennent des octaèdres à Ti et des groupes de disilicate [Si<sub>2</sub>O<sub>7</sub>]. Le feuillet *O* de la delindéite contient un polyèdre volumineux à (Na,K) de même que des sites Na et Ti octaédriques. Les polyèdres à alcalins sont partiellement vides. Le Ba est situé dans l'interfeuillet. Nous évaluons l'évidence d'un lessivage des alcalins, le désordre atomique qui en résulte, et la position de la delindéite au sein de la série polysomatique de la bafertisite. En termes généraux, la série revêt un caractère méro-plésiotypique. En fait, les couches hétérophyllosilicatées *HOH* représentent *grosso modo* le module commun aux membres de cette série, tandis que le contenu interfoliaire est variable (mérotypisme) et peut modifier sa structure dans les différents membres de la série (plésiotypisme).

(Traduit par la Rédaction)

*Mots-clés:* delindéite, structure cristalline, série polysomatique de la bafertisite, titanosilicates, hétérophyllosilicates, mérotypisme, plésiotypisme.

<sup>§</sup> E-mail address: ferraris@dsmp.unito.it

## INTRODUCTION

In spite of their large diversity, natural titanosilicates are rare minerals. They seem restricted to hyperagpaitic pegmatites and to hydrothermally and metasomatically modified rocks enriched in lithophile elements (Khomyakov 1995). Of about 30 known titanosilicates, 16 contain Ba and belong to the heterophyllosilicate family, a group of layer silicates discussed below and based on a structural *HOH* layer comparable to the *TOT* layer of the phyllosilicates (Ferraris 1997, Ferraris *et al.* 1996b). In fact, according to the usually adopted (001) orientation, the *HOH* heterophyllosilicate layer is obtained from the *TOT* layer by substituting selected [100] rows of disilicate groups ( $\text{Si}_2\text{O}_7$ ) by "hetero" rows of Ti-octahedra in the *T* sheet (Fig. 1); the resulting sheet is labeled *H*, but a different polysomatic interpretation has been proposed by Christiansen *et al.* (1999). Depending on the [010] periodicity of the substitution, three types of *HOH* layers are so far known: nafertisite (Ferraris *et al.* 1996a), astrophyllite and bafertisite, in order of decreasing [010] periodicity and ratio of Ti-octahedra to Si-tetrahedra in the *H* sheet (Ferraris 1997). The bafertisite type is the most widely represented, as it includes about 30 minerals, as discussed below. As with phyllosilicates, heterophyllosilicates may exhibit polytypism, as discussed, for example, by Christiansen *et al.* (1999).

Among Ba titanosilicates, delindeite is one of the rarest minerals. So far, only two occurrences are known and, in both cases, the amount of collected material is insignificant. Delindeite was firstly described (Appelman *et al.* 1987) from cavities of nepheline syenites at the Diamond Jo quarry in southern part of the Magnet Cove alkaline complex, Arkansas. There, the mineral occurs as spherulites up to 1 mm in diameter, consisting of pinkish grey lamellae, in a hydrothermal assemblage together with pyroxene, titanite, pectolite, barite, sphalerite, K-feldspar, labuntsovite, and lourenswalsite. Later, delindeite was found at Mt. Yukspor, Khibina alkaline complex, Kola Peninsula, Russia (Khomyakov 1995), where it occurs as dark cherry-colored small tablets, up to 2 mm in length. These tablets form rosette-like aggregates within cavities of a rischorritic pegmatite, together with shcherbakovite, lamprophyllite, wadeite, umbite, and kostylevite, among others. Chemical, optical, and X-ray powder-diffraction data as well as the density have been obtained for delindeite from both localities. From electron-diffraction data, a monoclinic symmetry with possible space-group *C2/m* (*a* and *b* interchanged in the present study), and unit-cell parameters were determined for the Magnet Cove mineral. Appelman *et al.* (1987) gave the following formula:  $(\text{Na,K})_{2.7}(\text{Ba,Ca})_4(\text{Ti,Fe,Al})_6\text{Si}_8\text{O}_{26}(\text{OH})_{14}$  ( $Z = 1$ ;  $D_{\text{obs}} 3.30 \text{ g/cm}^3$ ;  $D_{\text{calc}} 3.70 \text{ g/cm}^3$ ). For delindeite from Khibina, Khomyakov (1995) gave an ideal formula  $\text{Na}_2\text{Ba}_2\text{Ti}_3\text{Si}_4\text{O}_{16}(\text{OH,F})_2$  ( $Z = 2$ ;  $D_{\text{obs}} 3.45 \text{ g/cm}^3$ ).

The crystal structure of delindeite has not yet been established owing to splitting of the available crystals, presumably because of an easy {001} cleavage (present orientation). Recently, a third occurrence of delindeite was discovered at the Kirovskii apatite mine, Khibina complex, by amateur mineralogist A.S. Podlesnyi. At this new locality, delindeite occurs together with aegirine, biotite, and carbonate-fluorapatite in cavities within thin natrolite veinlets cross-cutting urtite. The mineral forms pinkish brown rectangular tablets up to  $0.6 \times 0.3 \text{ mm}$ . These tablets also are usually split, but it has been possible to select one single crystal suitable for an XRD study, the results of which are reported in this paper.

## EXPERIMENTAL

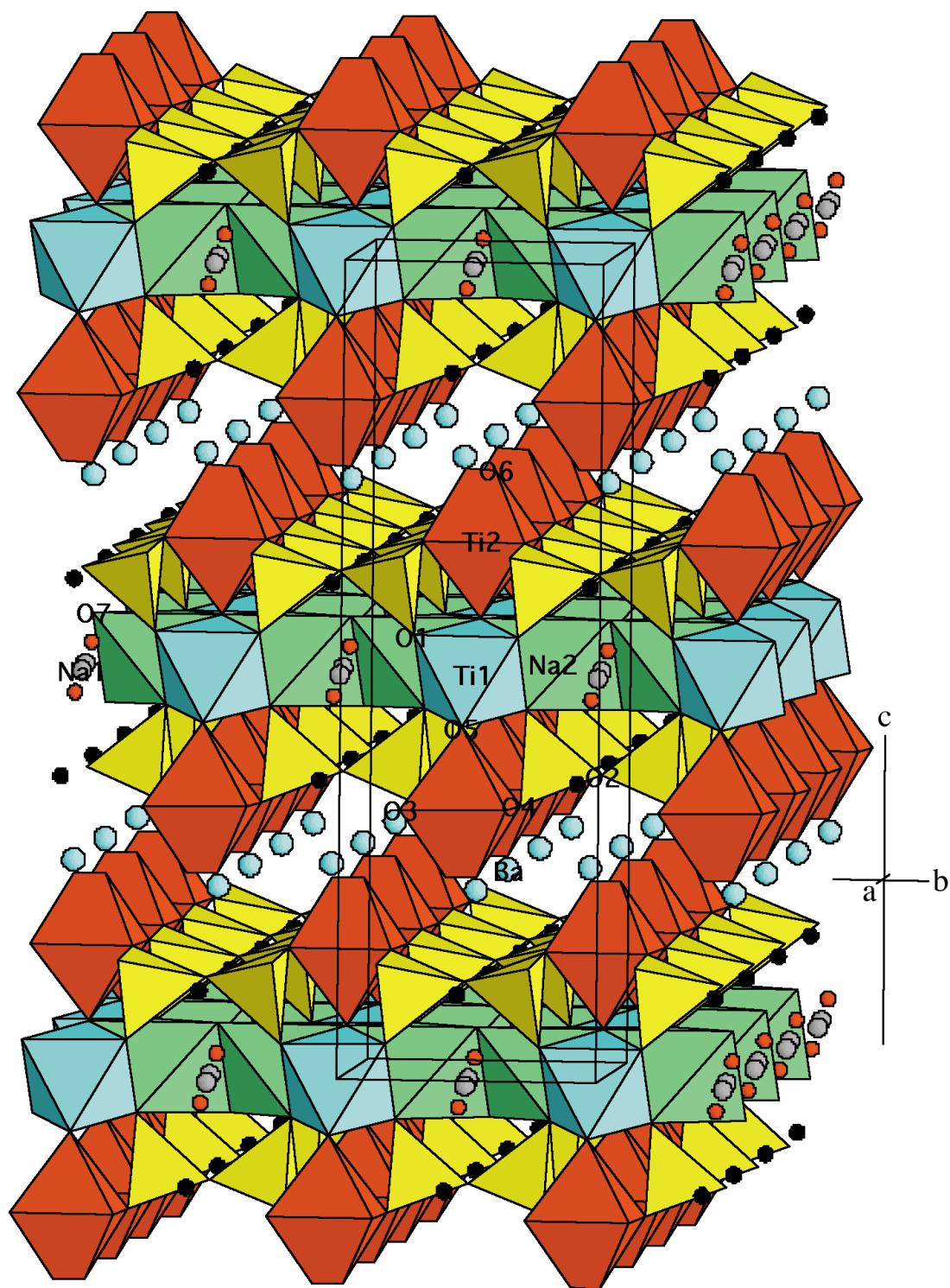
The results of the electron-microprobe analyses are summarized in Table 1. They were obtained at the Department of Geology, Moscow State University, with a Camebax SX-50 instrument [operating conditions: 20 kV (15 kV for Na), 20 nA, electron beam  $10 \times 10 \mu\text{m}$ ; analyst: N.N. Kononkova]. Taking  $\text{H}_2\text{O}$  by difference, the following empirical formula has been calculated on

TABLE 1. AVERAGE CHEMICAL COMPOSITION OF DELINDEITE FROM THE KIROVSKII MINE, Khibina COMPLEX

Oxides		Range	Standard
$\text{Na}_2\text{O}$ wt%	4.82	4.64 – 4.87	albite
$\text{K}_2\text{O}$	1.04	0.83 – 1.24	orthoclase
$\text{CaO}$	0.04	0.03 – 0.05	andradite
$\text{SrO}$	0.29	0.28 – 0.31	$\text{SrSO}_4$
$\text{BaO}$	34.46	34.11 – 34.92	$\text{BaSO}_4$
$\text{MnO}$	0.37	0.13 – 0.58	$\text{MnTiO}_3$
$\text{ZnO}$	0.09	0.00 – 0.26	$\text{ZnO}$
$\text{Fe}_2\text{O}_3^*$	2.93	1.85 – 4.15	andradite
$\text{Al}_2\text{O}_3$	0.48	0.33 – 0.71	albite
$\text{SiO}_2$	26.10	25.60 – 26.91	andradite
$\text{TiO}_2$	23.01	21.66 – 24.12	$\text{MnTiO}_3$
$\text{Nb}_2\text{O}_5$	0.39	0.21 – 0.59	$\text{LiNbO}_3$
$\text{H}_2\text{O}^{**}$	5.98		
Total	100.00		

\* The total Fe is expressed as  $\text{Fe}^{3+}$ . \*\* By difference. The composition is the average result of four electron-microprobe analyses done on two grains. Mg, Zr and F were not detected.

FIG. 1. Perspective view of the delindeite structure. Blue, red and green octahedra represent Ti(1), Ti(2) and Na(2) polyhedra, respectively. Grey and light blue circles represent Na(1) and Ba atoms, respectively. The alternative disordered positions of Na(1), bridging O(2) (black circles) and  $\text{H}_2\text{O}$  oxygen O(7) (red circles) are shown. The disordered position of O(6) results in a doubled corner of the Ti(2) octahedron.



the basis of  $\text{Si} + \text{Al} = 4$ :  $(\text{Na}_{1.40}\text{K}_{0.20}\text{Sr}_{0.02}\text{Ca}_{0.01})_{\Sigma 1.63}\text{Ba}_{2.02}(\text{Ti}_{2.60}\text{Fe}^{3+}_{0.33}\text{Mn}^{2+}_{0.05}\text{Nb}_{0.03}\text{Zn}_{0.01})_{\Sigma 3.02}(\text{Si}_{3.91}\text{Al}_{0.09})_{\Sigma 4.00}\text{O}_{15.26}(\text{OH})_{2.74} \cdot 1.62\text{H}_2\text{O}$ . Considering the brown color of crystals and the Fe-for-Ti substitution (see crystal structure), Fe has been taken as  $\text{Fe}^{3+}$ . The ratio of OH to O is calculated from the charge balance. The value of  $D_{\text{calc}}$  based on the crystal-chemical formula shown is  $3.82 \text{ g/cm}^3$  ( $Z = 2$ ). As already found by Appleman *et al.* (1987), this value is significantly greater than the measured values available in literature. We contend that as the grains of delindeite are split, they contain empty space. Owing to the very small dimensions and splitting of the grains, we could not obtain an experimental value of the density on the Kirovskii material. On structural grounds (see below), the ideal formula of delindeite is:  $\text{Ba}_2\{(\text{Na}, \text{K}, \square)_3(\text{Ti}, \text{Fe})[\text{Ti}_2(\text{O}, \text{OH})_4\text{Si}_4\text{O}_{14}](\text{H}_2\text{O}, \text{OH})_2\}$ .

A total of 5018 reflections were collected with a single-crystal X-ray diffractometer (details in Table 2), assuming a *P* lattice. The unit-cell parameters  $a$  5.327(2),  $b$  6.856(2),  $c$  21.51(3) Å,  $\beta$  93.80(4)° were obtained by least-square refinement of 13 reflections in the range  $15 \leq 2\theta \leq 30^\circ$ . The  $a$  and  $b$  parameters given in literature are interchanged in order to maintain the (001) orientation of the HOH layer, consistent with the bafertsite series. The crystal structure was solved by direct methods and refined isotropically in the space group *A2/m* using 703 observed independent reflections with  $I > 2\sigma(I)$  (SHELX-97 package; Sheldrick 1997) to  $R(F) = 0.143$ . The anisotropic refinement converged to  $R(F) = 0.054$  for 703 independent reflections with  $I > 2\sigma(I)$ . The refinement was isotropic for the split atoms Ba' and Ba". A table with the values of the anisotropic displacement parameters is deposited. Negative aniso-

tropic displacement parameters obtained for O6 and splitting of some atomic positions could be interpreted as an indication of a lower symmetry. Therefore, the structure was solved and refined also in space groups *A2* and *Am*. We obtained, for 1269 independent reflections with  $I > 2\sigma(I)$ ,  $R(F) = 0.057$  and 0.062, respectively. These acentric models also tested negatively for twinning by merohedry. However, anomalous positional parameters obtained during the refinement in these space groups, namely short Si-O (~1.49 Å) and Ti-O (~1.78 Å) distances, and negative anisotropic thermal displacement parameters for most of the atoms, led us to prefer space group *A2/m*. On the whole, the poor  $R_{\text{int}}$  value (0.11) obtained by merging the 5018 measured reflections and the consequent relatively high  $R$  value can be attributed to the poor quality of the only crystal available. Information on data collection and refinement, atomic coordinates and equivalent thermal displacement parameters, selected interatomic distances, and results of bond-strength calculations are reported in Tables 2, 3, 4, and 5, respectively. A table of structure factors is available at the Depository of Unpublished Data, CISTI, National Research Council, Ottawa, Ontario K1A 0S2, Canada.

## RESULTS AND DISCUSSION

### The structure

The structure of delindeite is characterized by positional disorder at Ba, Na(1), O(2), O(6) and O(7) sites (Table 3), and partial vacancy at the O(6) and Na(2) sites. The two statistically occupied positions Na(1) and O(6) are related by a center of inversion and a mirror

TABLE 2. INFORMATION ON COLLECTION AND REFINEMENT OF DATA ON DELINDEITE

Chemical formula	$\text{Ba}_2\{(\text{Na}, \text{K}, \square)_3(\text{Ti}, \text{Fe})[\text{Ti}_2(\text{O}, \text{OH})_4\text{Si}_4\text{O}_{14}](\text{H}_2\text{O}, \text{OH})_2\}$
Unit formula weight	1801.16
Radiation and wavelength	MoK $\alpha$ , 0.71069 Å
$\mu$	6.89 mm <sup>-1</sup>
Equipment	Siemens P4 diffractometer, graphite monochromator
Space group; Z	<i>A2/m</i> ; 2
Unit-cell dimensions	$a$ 5.327(2), $b$ 6.856(2), $c$ 21.51(3) Å, $\beta$ 93.80(4)°
Unit-cell volume	783.96 Å <sup>3</sup>
$F(000)$	836
$D(\text{calc.})$	3.82 g/cm <sup>3</sup>
$D(\text{obs.})^*$	3.45 g/cm <sup>3</sup>
Crystal size	0.14 × 0.10 × 0.03 mm
Index ranges	-25 ≤ $h$ ≤ 25, -8 ≤ $k$ ≤ 8, -6 ≤ $l$ ≤ 6
Standard reflection	every 100 reflections
Collected reflections	5018
Ind. reflections with $I > 2\sigma(I)$	703; $R_{\text{int}} = 0.11$
Refinement method	full-matrix least-squares on $F^2$
Weights	$1/[\sigma(F_o)^2 + (0.060P)^2 + (24.0P)]$ , $P = [\max(F_o)^2 + 2(F_c)^2]$
$R(F)$ , $R(F^2)$ , Goof	0.054; 0.142; 1.114
Number of refined parameters	119
Largest residues ( $e/\text{Å}^3$ )	2.17; -1.66

\* Value quoted by Khomyakov (1995); see text.

TABLE 3. ATOMIC COORDINATES, EQUIVALENT ISOTROPIC DISPLACEMENT PARAMETERS ( $U_{\text{eq}}$ )<sup>§</sup> AND SITE-OCCUPANCY COEFFICIENTS (WHERE REFINED) FOR DELINDEITE

Atom	$x$	$y$	$z$	Sof	$U_{\text{eq}}$ (Å <sup>2</sup> )
Ba	0.2539(2)	0	0.27141(4)	0.96(1)	0.017(1)
Ba'	0.254(7)	0	0.221(2)	0.02(1)	0.015
Ba"	0.261(8)	0	0.320(2)	0.02(1)	0.015
Ti(1)*	0	0	0		0.015(1)
Ti(2)	0.2731(6)	½	0.3453(2)		0.057(2)
Si	0.7891(7)	-0.2298(4)	0.3788(1)		0.020(1)
Na(1)**	-0.055(5)	0	0.503(3)	0.24(1)	0.029(9)
Na(2)	½	-0.246(2)	½	0.56(2)	0.030(3)
O(1)	0.827(2)	-0.299(1)	0.4510(4)		0.029(2)
O(2)	0.097(3)	0	0.6252(9)	0.54(1)	0.022(6)
O(2')	0.326(4)	0	0.616(1)	0.46(1)	0.032(7)
O(3)	0.527(2)	-0.297(2)	0.3461(5)		0.061(4)
O(4)	0.012(2)	-0.302(2)	0.3399(5)		0.072(5)
O(5)	-0.272(2)	0	0.0596(5)		0.028(3)
O(6)	0.260(2)	0.059(2)	0.7577(7)	0.50(3)	0.022(5)
O(7)W	0.287(5)	0	0.440(2)	0.58(2)	0.048(7)
O(7')W	0.252(9)	0	0.476(3)	0.38(1)	0.032(7)

\* Includes Fe. \*\* Includes K. Numbers in parentheses are estimated standard deviations referred to the last digit. § (fixed  $U_{\text{eq}}$  for Ba' and Ba").

TABLE 4. SELECTED INTERATOMIC DISTANCES (Å)  
IN THE STRUCTURE OF DELINDEITE

Ba – O(3)	2.92(1) × 2	Ti(2) – O(5)	2.03(1)
– O(4)	2.89(1) × 2	– O(3)	1.95(1) × 2
– O(4)	3.03(1) × 2	– O(4)	1.95(1) × 2
– O(2)	3.01(2)	– O(6)	1.91(2)
[– O(2')]	3.19(1)]		
– O(6)	3.04(1)	Na(1) – O(1)	2.40(3) × 2
– O(6)	2.80(1)	– O(1)	2.56(3) × 2
– O(6)	2.74(1)	– O(2)	2.69(7)
		– O(2)	2.74(7)
Ba' – O(4)	2.32(3) × 2	[– O(2')]	2.99(1)
– O(3)	2.37(3) × 2	– O(2')	2.82(6)]
– O(6)	2.63(4)	– O(7)	2.33(5)
– O(6)	2.83(4)		
		Na(2) – O(1)	2.125(9) × 2
Ba'' – O(4)	2.51(3) × 2	– O(5)	2.44(1) × 2
– O(3)	2.52(3) × 2	– O(7)	2.34(2) × 2
– O(2')	2.53(5)	[– O(7')]	2.18(3) × 2]
– O(7)	2.58(5)		
		Si – O(1)	1.618(8)
Ti(1) – O(1)	1.936(8) × 4	– O(3)	1.587(9)
– O(5)	2.01(1) × 2	– O(4)	1.57(1)
		– O(2)	1.693(6)
		[– O(2')]	1.697(7)]

The numbers in parentheses are estimated standard deviations referred to the last digit. For the Ba' and Ba'' positions, which are alternative to Ba, only Ba – O bonds shorter than 3 Å are given.

plane, respectively [Na(1) – Na(1') = 0.61(6) Å; O(6) – O(6') = 0.81(3) Å]. According to the site-occupancy factors (sof) shown in Table 3, Na(1) and O(6) account for 0.96 and 4 atoms per cell, respectively. Both O(2)

and O(7) are split between two independent positions [O(2) – O(2') = 1.25(3) Å; O(7) – O(7') = 0.79(5) Å] and, according to their site-occupancy factor, they account for 4 and 3.8 atoms per cell, respectively. Ba occupies mainly (96%) one position, but a plot of electron density showed two additional sites, Ba' and Ba'' 2% occupied, at 1.05(4) and 1.08(4) Å from the main Ba site. From Table 4, one can see that these low-occupancy Ba positions are shifted toward those oxygen atoms that establish long bonds with the main Ba position. In addition to the Na(1) site, the Na(2) site also is partially vacant; for both Na sites, the site-occupancy values reported in Table 3 have been obtained by using the scattering curve of Na. The total of about 47% alkali vacancy indicated by the refinement of Na(1) and Na(2) is in good agreement with the results of chemical analysis, which show a deficiency of 1.4 out of 3 alkali atoms per formula unit (Table 1).

The larger dimension of the Na(1) polyhedron [ $\langle \text{Na-O} \rangle$  2.52 and 2.58 Å, where O(2) and O(2') are the ligands of Na, respectively] in comparison to that of the Na(2) polyhedron [ $\langle \text{Na-O} \rangle$  2.31 and 2.25 Å, where O(7) and O(7') are the ligands of Na, respectively] suggests that the amount of K (plus the small amount of Sr and Ca) found by chemical analysis resides at the Na(1) site. The refinement of electron density at the two Ti sites shows that all Fe enters the Ti(1) site, which belongs to the ideally octahedral O sheet of the HOH layer (see below). This finding is in accordance with the generally observed preference of Ti for the octahedral sites

TABLE 5. RESULTS OF BOND-STRENGTH CALCULATIONS FOR DELINDEITE

	Ba	Ti(1)	Ti(2)	Si	Na(1)	Na(2)	Σ
O(1)		<i>0.73</i> × 4	0.73	1.00	<i>0.05</i> × 2	0.05	2.04
					<i>0.03</i> × 2	0.03	
O(2) [O(2')]	0.12			<i>0.83</i>	0.83 × 2	0.02; 0.02	1.82
O(3)	<i>0.18</i> × 2	0.18	<i>0.71</i> × 2	0.71			1.99
O(4)	<i>0.19</i> × 2	0.19	<i>0.71</i> × 2	0.71			2.17
	<i>0.14</i> × 2	0.14					
O(5)*		<i>0.61</i> × 2	0.61	0.53		0.10 × 2	1.34
O(6)*	0.29; 0.25; 0.13		0.73				1.40
O(7) W [O(7')]					0.08	0.16 × 2	0.40
Σ	1.81	4.14	4.10	4.06	0.28	0.98	

\* [O<sub>0.45</sub>(OH)<sub>0.55</sub>]. Contribution to the balance of cations is in italics.

that replace the disilicate groups to form an *H* sheet (see Introduction). The cation substitutions and deficiencies are charge-balanced mainly by the  $O^{2-} \rightarrow (OH)^-$  substitution at the O(5) and O(6) sites (see below).

The crystal structure of delindeite is based on the (001) *HOH* bafertisite-like module mentioned in the Introduction. As discussed by Ferraris (1997), the oxygen atoms in bafertisite-like structures that are not bonded to Si do not necessarily represent  $O^{2-}$ , but they can also either be  $(OH)^-$  or  $(H_2O)^0$ . Owing to the atomic disorder described and the consequent presence of alternative coordination polyhedra, the calculation of bond strengths cannot accurately be done. In any case, the values of bond strengths, calculated according to Brown & Shannon (1973), clearly indicate that O(5) and O(6) consist of OH groups in about 50% of the cases, and O(7) is mainly a  $H_2O$  molecule (Table 5). A hydrogen-bonding scheme for these H-carrying oxygen atoms cannot clearly be established because they are not involved in O...O contacts shorter than  $\sim 3$  Å. Presumably the underbonded O(2) (Table 5) is hydrogen-bonded to O(6), and the  $H_2O$  oxygen O(7) is hydrogen-bonded with symmetry-related O(7) positions. O(5) and O(7) are the only two oxygen atoms belonging to the octahedral *O* sheet that are not bonded to Si (Table 4,

Figs. 1, 2); O(6), on the other hand, occupies the doubled corner of the Ti(2) octahedron that points toward the interlayer (Fig. 1).

#### Disorder and leaching

The structure of our sample and the known chemical compositions of delindeite reported above show that this titanosilicate is cation-deficient with respect to the ideal formula of bafertisite-like phases (see below). The structural disorder and the lack of good crystals support the hypothesis that the cation deficiency is due to alkali leaching, a situation to be compared, *e.g.*, with that reported for steenstrupine-(Ce) (Makovicky & Karup-Møller 1981). The leaching affects sites in the *O* sheet of the *HOH* layer, a quite unusual situation for a layer structure, where the more weakly bonded cations reside in the interlayer. Thus, vacancies in the *O* sheet require charge balance (*e.g.*, the mentioned  $O^{2-} \rightarrow OH$  substitution) and substantial readjustment within the layer, such as the splitting of O(2) and O(7) that are coordinated by the Na sites (Table 4). Note that unlike most titanosilicates, where the *O* sheet is occupied by typical octahedrally coordinated cations such as Fe, Mn and Mg, two independent Na sites occur in the *O* sheet of

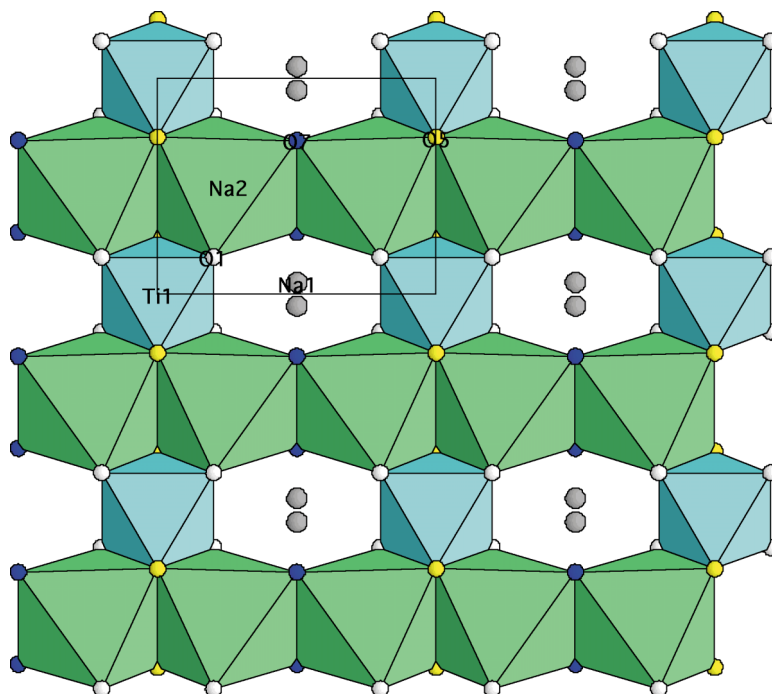


FIG. 2. "Octahedral" *O* sheet in delindeite. Colors of polyhedra as if Figure 1; the two disordered positions of Na(1) are shown.

delindeite. Whereas Na(2) occupies a normal octahedral site within the *O* sheet, Na(1) is coordinated not only to O(1), the apical oxygen of the tetrahedron, but also to the bridging oxygen O(2). In an ideal *HOH* layer, the latter oxygen atom would be basal in the Si-tetrahedron; instead, in delindeite, this oxygen atom also is within the large coordination sphere of Na(1). The statistical distribution of O(2) on two independent positions avoids the strain of an O...O edge shared between an *H* and an *O* sheet. A similar coordination for the bridging oxygen also has been reported in the structure of a Ca-rich seidozerite (Skszat & Simonov 1966).

The splitting of O(6), on the other hand, is probably related to the necessity of assuring a more uniform distribution of anions around the large interlayer cation Ba (Table 4), which site, in turn, is found slightly to be split. The presence of such a large cation can also explain why in delindeite the Ti-octahedra of two heterophyllosilicate sheets facing across the interlayer do not share a corner [O(6) in this case], as for example happens in triclinic astrophyllite (Yamnova *et al.* 2000), nafertisite (Ferraris *et al.* 1996a) and perraultite (Yamnova *et al.* 1998). Note that in other titanosilicates, *e.g.*, monoclinic astrophyllite (Shi *et al.* 1998), this corner is missing because Ti has coordination 5. In seidozerite (Simonov & Belov 1960), in contrast, an edge is shared by two facing Zr-octahedra.

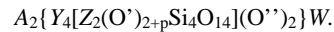
#### *The bafertisite mero-plesiotype series*

Ferraris *et al.* (1996b), Ferraris (1997), Egorov-Tismenko (1998) and Christiansen *et al.* (1999) considered the modular aspects of a large group of about 20 titanosilicates that may contain bafertisite-type *HOH* layers similar to those found in delindeite. For compounds with unknown structure, inclusion in the group by Ferraris (1997) was based on cell parameters and chemical data. This approach is consistent with the structural application of modularity concepts (Ferraris 1997, Merlino 1997) and the prediction has been confirmed in those cases (lamprophyllite-group phases, delindeite, perraultite, bornemanite, bussenite) for which the structure was later determined (Table 6). An updated list of these structures is given in Table 6 following the same criteria.

All the titanosilicates listed in Table 6 are characterized by similar values of  $a \approx 5.5 \text{ \AA}$  and  $b \approx 7 \text{ \AA}$  parameters, which are typical of the bafertisite *HOH* module mentioned in the Introduction. As in layer silicates, two adjacent *HOH* modules [see Ferraris (1997) for details] define an interlayer space that may contain either a single cation or an entire mineral-forming module. The latter is the case of quadrophylite and polyphite (Khomyakov *et al.* 1992), where a module of the species nacaphite (Sokolova *et al.* 1989) is present. The interlayer content determines the value of the *c* parameter which, of course, increases with the complexity of the sandwiched module (Table 6). On its own, the thick-

ness of the *HOH* layer is about  $10 \text{ \AA}$ . Where the interlayer is simple, the *c* parameter is close to  $n \times 10 \text{ \AA}$ , with *n* indicating the number of independent *HOH* layers. In Table 6, minerals are listed in order of the increasing parameter  $t = d(001)/n$  and, implicitly, in order of increasing complexity of the chemical formula. In bornemanite, modules of both seidozerite and lomnosovite occur; thus the value of *t* no longer directly indicates the complexity of the interlayer content (Ferraris *et al.* 2002).

Ferraris (1997) proposed the following general formula for the bafertisite-like titanosilicates:



In this formula,  $[Z_2(O')_{2+p}Si_4O_{14}]^{n-}$  is a complex anion representing the heterophyllosilicate *H* sheet;  $\{Y_4[Z_2(O')_{2+p}Si_4O_{14}](O'')_2\}^{m-}$  is a complex anion representing the heterophyllosilicate *HOH* layer, and is shown within braces to emphasize the interlayer content *A* and *W* (Table 6). In the formula, O' and O'' represent oxygen atoms not bonded to Si. They may represent  $O^{2-}$ ,  $(OH)^-$  or  $(H_2O)^0$ ; in particular, O' is bonded to Z (one O' corresponds to the corner pointing into the interlayer space and is labeled *C* below).

Furthermore, *A* represents the large interlayer cations, and *W*, the (complex) interlayer content (cations, anions,  $H_2O$ ) other than *A*; *Y* represents the cations forming the *O* sheet, and *Z*, the cations occupying the heterophyllosilicate polyhedron (usually an octahedron) belonging to the *H* sheet. The variable *p* may adopt a value of 2 or 1 depending on whether the *Z* octahedron does not or does share its corner *C*;  $p = 0$  where *Z* has (i) coordination 5, (ii) *C* is shared with an interlayer anion, and (iii) the *Z*-octahedron shares an edge.

On the basis of Makovicky's (1997) definition and further discussion in Christiansen *et al.* (1999) of the merotype series (both common and peculiar modules are present in the members of the series) and plesiotype series (the component modules of the series may differ for some parts in specific members), the titanosilicates given in Table 6 form a mero-plesiotype series, which we call the bafertisite (polysomatic) series. This series is considered merotype because one module, namely the layer *HOH*, is uniformly present (but see below) in all members, and a second module, namely the interlayer part (*A* + *W*), is peculiar for each member. At the same time, the bafertisite series has a plesiotype character because the *HOH* layer modifies not only its chemical composition but, more importantly, commonly also changes to some extent its topology, including the coordination number of the *Z* cation, which can be either 5 or 6. Delindeite is a typical example to illustrate the plesiotype character of the series; in fact, the *O* sheet is not strictly octahedral because Na(1) coordinates also O(2) which, in an ideal *HOH* layer, should be a basal oxygen of the Si-tetrahedra.

TABLE 6. MEMBERS OF THE MERO-PLESIOTYPE SERIES  
IN ORDER OF INCREASING THICKNESS  $t = d(001)n$ ,  
WITH  $n$  CORRESPONDING TO THE NUMBER OF *HOH* LAYERS IN THE CELL

Mineral	Formula	$t$ (Å)	Reference*
Seidozerite	$\text{Na}_2\{(\text{Na}, \text{Mn}, \text{Ti})_4[(\text{Zr}, \text{Ti})_2\text{O}_2\text{Si}_4\text{O}_{14}]\text{F}_2\}$	8.93	Simonov & Belov (1960)
Lamprophyllite	$(\text{Sr}, \text{K}, \text{Ba})_2\{(\text{Na}, \text{Na}, \text{Fe})_2\text{Ti}[\text{Ti}_2\text{O}_2\text{Si}_4\text{O}_{14}](\text{O}, \text{OH})_2\}$	9.68	Rastsvetaeva <i>et al.</i> (1990)
Barytolamprophyllite	$(\text{Ba}, \text{Na})_2\{(\text{Na}, \text{Ti}, \text{Fe}, \text{Ba})_4[\text{Ti}_2\text{O}_2\text{Si}_4\text{O}_{14}](\text{OH}, \text{F})_2\}$	9.80	Peng <i>et al.</i> (1984)
Orthoericssonite	$(\text{Ba}, \text{Sr})_2\{(\text{Mn}, \text{Fe})_4[\text{Fe}_2\text{O}_2\text{Si}_4\text{O}_{14}](\text{OH})_2\}$	10.11	Matsubara (1980)
Ericssonite**	$\text{Ba}_2\{\text{Mn}_4[\text{Fe}_2\text{O}_2\text{Si}_4\text{O}_{14}](\text{OH})_2\}$	10.16	Moore (1971)
Shkatalukite**	$(\text{Na}, \square)_2\{(\text{Na}, \text{Mn}, \text{Ca}, \square)_4[(\text{Ti}, \text{Nb})_2(\text{O}, \text{OH})_2\text{Si}_4\text{O}_{14}](\text{OH}, \text{F})_2\} \cdot \text{H}_2\text{O}$	10.34	Men'shikov <i>et al.</i> (1996)
Jinshajiangite**	$(\text{Na}, \text{Ca})(\text{Ba}, \text{K})\{(\text{Fe}, \text{Mn})_4[(\text{Ti}, \text{Nb})_2\text{O}_2\text{Si}_4\text{O}_{14}](\text{F}, \text{O})_2\}$	10.37	Hong & Fu (1982)
Perraultite	$(\text{Na}, \text{Ca})(\text{Ba}, \text{K})\{(\text{Mn}, \text{Fe})_4[(\text{Ti}, \text{Nb})_2\text{O}_2\text{Si}_4\text{O}_{14}](\text{OH}, \text{F})_2\}$	10.38	Yamnova <i>et al.</i> (1998)
Delindeite	$\text{Ba}_2\{(\text{Na}, \square)_3\text{Ti}[\text{Ti}_2(\text{O}, \text{OH})_2\text{Si}_4\text{O}_{14}](\text{H}_2\text{O}, \text{OH})_2\}$	10.73	This study
Bafertisit	$\text{Ba}_2\{(\text{Fe}, \text{Mn})_4[\text{Ti}_2\text{O}_2(\text{O}, \text{OH})_2\text{Si}_4\text{O}_{14}](\text{O}, \text{OH})_2\}$	10.85	Guan <i>et al.</i> (1963)
Hejmanite	$\text{Ba}_2\{(\text{Mn}, \text{Fe})_4[\text{Ti}_2(\text{O}, \text{OH})_2\text{Si}_4\text{O}_{14}](\text{OH}, \text{F})_2\}$	10.90 <sup>§</sup>	Rastsvetaeva <i>et al.</i> (1991)
Murmanite	$\text{Na}_2\{(\text{Ti}, \text{Na}, \square)_4[\text{Ti}_2\text{O}_2(\text{O}, \text{OH})_2\text{Si}_4\text{O}_{14}](\text{O}, \text{OH})_2\}$	11.60	Khalilov (1989)
Epistolite**	$\text{Na}_2\{(\text{Na}_3\text{Ti})[(\text{Nb}, \text{Ti})_2\text{O}_2(\text{O}, \text{OH})_2\text{Si}_4\text{O}_{14}](\text{O}, \text{F})_2\}$	11.92	Khalilov <i>et al.</i> (1965)
Bornemanite	$\text{Na}_2\text{Ba}\{(\text{Na}, \text{Ti}, \text{Mn})_4[(\text{Ti}, \text{Nb})_2\text{O}_2\text{Si}_4\text{O}_{14}](\text{F}, \text{OH})_2\}\text{PO}_4$	11.99	Ferraris <i>et al.</i> (2001)
Vuonnemite	$\text{Na}_6\{(\text{Na}, \text{Ti})_4[\text{Nb}_2\text{O}_2\text{Si}_4\text{O}_{14}](\text{O}, \text{OH}, \text{F})_2\}(\text{PO}_4)_2$	14.40	Ercit <i>et al.</i> (1998)
Lomonosovite	$\text{Na}_8\{(\text{Na}, \text{Ti})_4[\text{Ti}_2\text{O}_2\text{Si}_4\text{O}_{14}](\text{O}, \text{F})_2\}(\text{PO}_4)_2$	14.48	Belov <i>et al.</i> (1978)
Innelite	$(\text{Ba}, \text{K})_2\text{Ba}_2\{(\text{Na}, \text{Ca})_3\text{Ti}[\text{Ti}_2\text{O}_2\text{Si}_4\text{O}_{14}]\text{O}_2\}(\text{SO}_4)_2$	14.65	Chernov <i>et al.</i> (1971)
Yoshimuraite	$\text{Ba}_4\{\text{Mn}_4[\text{Ti}_2\text{O}_2\text{Si}_4\text{O}_{14}](\text{OH})_2\}(\text{PO}_4)_2$	14.74	McDonald <i>et al.</i> (2000)
Busenite***	$\text{Na}_2(\text{Ba}, \text{Sr}, \text{Ca}, \text{K})_4\{(\text{Na}, \text{Fe}, \text{Mn})_4[\text{Ti}_2(\text{OH})_4\text{Si}_4\text{O}_{14}]\}(\text{CO}_3)_2(\text{OH})_2\text{F}_2$	15.85	Khomyakov <i>et al.</i> (2001)
Quadruphite	$\text{Na}_{13}\text{Ca}\{(\text{NaMgTi}_2)[\text{Ti}_2\text{O}_2\text{Si}_4\text{O}_{14}]\text{O}_2\}(\text{PO}_4)_2\text{F}_2$	20.25	Khomyakov <i>et al.</i> (1992)
Sobolevit	$\text{Na}_2\text{CaMg}\{(\text{NaMgTi}_2)[\text{Ti}_2\text{O}_2\text{Si}_4\text{O}_{14}]\text{O}_2\}(\text{PO}_4)_2\text{F}_2$	20.28	Sokolova <i>et al.</i> (1988)
Polyphite	$\text{Na}_{14}(\text{Ca}, \text{Mn}, \text{Mg})_3\{(\text{Ti}, \text{Mn}, \text{Mg})_4[\text{Ti}_2\text{O}_2\text{Si}_4\text{O}_{14}]\text{F}_2\}(\text{PO}_4)_6\text{F}_4$	26.49	Khomyakov <i>et al.</i> (1992)
M72**	$\text{BaNa}\{(\text{Na}, \text{Ti})[(\text{Ti}, \text{Nb})_2\text{O}_2\text{Si}_4\text{O}_{14}](\text{O}, \text{F})_2\} \cdot 4\text{H}_2\text{O}$	?	Khomyakov (1995)
M73**	$\text{BaNa}\{(\text{Na}, \text{Mn}, \text{Ti})_4[(\text{Ti}, \text{Nb})_2\text{O}_2\text{Si}_4\text{O}_{14}](\text{O}, \text{OH}, \text{F})_2\} \cdot 5\text{H}_2\text{O}$	?	Khomyakov (1995)
M55**	$(\text{Ba}, \text{K})_2\text{Na}_4\text{Ba}\{(\text{Ca}, \text{Nb}, \text{Mn}, \text{Fe})_4[\text{Ti}_2\text{O}_2\text{Si}_4\text{O}_{14}]\text{O}_2\}(\text{PO}_4)_2$	?	Khomyakov (1995)

\* Where the structure is known, the most recent description of the structure is referred to. \*\*Structure unknown.

\*\*\* M74 in Khomyakov (1995) and Ferraris *et al.* (1997). ? Cell unknown. <sup>§</sup> Phase II (space group *Cm*), which corresponds to the mineral hejmanite described by Vrána *et al.* (1992).

Note that the content of the heteropolyhedral *H* sheet is shown in square brackets, and that of the *HOH* layer is shown within braces; thus the composition of the interlayer is shown outside the braces.

A situation comparable with that occurring in the layer titanositates is found in the well-known 2:1 layer silicates, where both members without an interlayer content (talcs) and with an interlayer filled by a single cation (micas), octahedral layer (chlorites) and various kinds of interstratification (clays) occur.

#### ACKNOWLEDGEMENTS

The authors are grateful to referees E. Makovicky and S. Matsubara, Associate Editor O. Johnsen, and R.F. Martin for constructive critical comments that improved the text. This work was supported in part by the Russian Scientific Foundation (grants 99-05-39019, 00-05-65399, 00-15-96663), by bilateral Italian-Russian scientific cooperation program (project No. 62), and by the Russian Universities Program. D.Yu.P. benefitted from a NATO Guest Fellowship grant by CNR (Rome) and the University of Torino exchange program. The

contribution of G.F. and G.I. is in the framework of 40% MURST and CNR projects.

#### REFERENCES

- APPLEMAN, D.E., EVANS, H.T., JR., NORD, G.L., DWORNIK, E.J. & MILTON, C. (1987): Delindeite and lourensvalsite, two new titanositates from the Magnet Cove region, Arkansas. *Mineral. Mag.* **51**, 417-425.
- BELOV, N.V., GAVRILOVA, G.S., SOLOVIEVA, L.P. & KHALILOV, A.D. (1978): The refined structure of lomonosovite. *Sov. Phys. Dokl.* **22**, 422-424.
- BROWN, I.D. & SHANNON, R.D. (1973): Empirical bond strength - bond length curves for oxides. *Acta Crystallogr.* **A29**, 266-282.
- CHEKHOV, A.N., ILYUKHIN, V.V., MAKSIMOV, B.A. & BELOV, N.V. (1971): Crystal structure of innelite -  $\text{Na}_2\text{Ba}_3(\text{Ba}, \text{K}, \text{Mn})(\text{Ca}, \text{Na})\text{Ti}(\text{TiO}_2)_2(\text{Si}_2\text{O}_7)_2(\text{SO}_4)_2$ . *Sov. Phys. Crystallogr.* **16**, 65-69.



- CHRISTIANSEN, C.C., MAKOVICKY, E. & JOHNSEN, O. N. (1999): Homology and typism in heterophyllosilicates: an alternative approach. *Neues Jahrb. Mineral., Abh.* **175**, 153-189.
- EGOROV-TISMENKO, YU.K. (1998): On the seidozerite–nacaphite polysomatic series of minerals: titanosilicate analogues of mica. *Crystallogr. Rep.* **43**, 271-277.
- ERCIT, T.S., COOPER, M.A. & HAWTHORNE, F.C. (1998): The crystal structure of vuonnemite,  $\text{Na}_{11}\text{Ti}^{4+}\text{Nb}_2(\text{Si}_2\text{O}_7)(\text{PO}_4)_2\text{O}_3(\text{F},\text{OH})$ , a phosphate-bearing sorosilicate of the lomonosovite group. *Can. Mineral.* **36**, 1311-1320.
- FERRARIS, G. (1997): Polysomatism as a tool for correlating properties and structure. In *Modular Aspects of Minerals* (S. Merlino, ed.). *Eur. Mineral. Union, Notes in Mineral.* **1**, 275-295.
- \_\_\_\_\_, BELLUSO, E., GULA, A., SOBOLEVA, S.V., AGEEVA, O.A. & BORUTSKII, B.E. (2001): New data and structure model of the layer titanosilicate bornemanite based on seidozerite and lomonosovite modules. *Can. Mineral.* **39** (in press).
- \_\_\_\_\_, IVALDI, G., KHOMYAKOV, A.P., SOBOLEVA, S.V., BELLUSO, E. & PAVESE, A. (1996a): Nafertisite, a layer titanosilicate member of a polysomatic series including mica. *Eur. J. Mineral.* **8**, 241-249.
- \_\_\_\_\_, KHOMYAKOV, A.P., BELLUSO, E. & SOBOLEVA, S.V. (1996b): Polysomatic relationships in some titanosilicates occurring in the hyperagpaitic alkaline rocks of the Kola Peninsula, Russia. *Proc. 30<sup>th</sup> Int. Geol. Congress* **16**, 17-27.
- GUAN, YA. S., SIMONOV, V.I. & BELOV, N.V. (1963): Crystal structure of bafertisite,  $\text{BaFe}_2\text{TiO}[\text{Si}_2\text{O}_7](\text{OH})_2$ . *Dokl. Acad. Sci. USSR, Earth Sci. Sect.* **149**, 123-126.
- HONG WENXING & FU PINGJU (1982): Jinshajiangite – a new Ba-Mn-Fe-Ti-bearing silicate mineral. *Geochemistry (China)* **1**, 458-464 (in Chinese).
- KHALILOV, A.D. (1989): Refinement of the crystal structure of murmanite and data on its crystal-chemical properties. *Mineral. Zh.* **11**(5), 19-27 (in Russ.).
- \_\_\_\_\_, MAKAROV, E.S., MAMEDOV, K.S. & PYANSINA, L.YA. (1965): Crystal structures of minerals of the murmanite–lomonosovite group. *Dokl. Acad. Sci. USSR, Earth Sci. Sect.* **162**, 138-140.
- KHOMYAKOV, A.P. (1995): *Mineralogy of Hyperagpaitic Alkaline Rocks*. Clarendon Press, Oxford, U.K.
- \_\_\_\_\_, MEN'SHIKOV, YU. P., NECHELYUSTOV, G.N. & ZHOU HUYUN (2001): Bussenite  $\text{Na}_2\text{Ba}_2\text{FeTiSi}_2\text{O}_7(\text{CO}_3)(\text{OH})_3\text{F}$ , a new mica-like titanosilicate from the Khibina alkaline massif (Kola Peninsula). *Zap. Vser. Mineral. Obshchest.* **130**(3), 50-55 (in Russ.).
- \_\_\_\_\_, NECHELYUSTOV, G.N., SOKOLOVA, E.V. & DOROKHOVA, G.I. (1992): Quadruphite  $\text{Na}_{14}\text{CaMgTi}_4[\text{Si}_2\text{O}_7]_2[\text{PO}_4]_2\text{O}_4\text{F}_2$  and polyphite  $\text{Na}_{17}\text{Ca}_3\text{Mg}(\text{Ti},\text{Mn})_4[\text{Si}_2\text{O}_7]_2[\text{PO}_4]_6\text{O}_2\text{F}_6$ , two new minerals of the lomonosovite group. *Zap. Vser. Mineral. Obshchest.* **121**(3), 105-112 (in Russ.).
- MAKOVICKY, E. (1997): Modularity – different types and approaches. In *Modular Aspects of Minerals* (S. Merlino, ed.). *Eur. Mineral. Union, Notes in Mineralogy* **1**, 315-344.
- \_\_\_\_\_, & KARUP-MØLLER, S. (1981): Crystalline steenstrupine from Tunugdliarfik in the Ilímaussaq alkaline intrusion, South Greenland. *Neues Jahrb. Mineral., Abh.* **140**, 300-330.
- MATSUBARA, S. (1980): The crystal structure of orthoericssonite. *Mineral. J.* **10**, 107-121.
- MCDONALD, A.M., GRICE, J.D. & CHAO, G.Y. (2000): The crystal structure of yoshimuraite, a layered Ba–Mn–Ti silicophosphate, with comments of five-coordinated  $\text{Ti}^{4+}$ . *Can. Mineral.* **38**, 649-656.
- MEN'SHIKOV, YU.P., KHOMYAKOV, A.P., POLEZHAeva, L.I. & RASTSVETAeva, R.K. (1996): Shkatulkalite,  $\text{Na}_{10}\text{MnTi}_3\text{Nb}_3(\text{Si}_2\text{O}_7)_6(\text{OH})_2\text{F}\cdot 12\text{H}_2\text{O}$ : a new mineral. *Zap. Vser. Mineral. Obshchest.* **125**(1), 120-126 (in Russ.).
- MERLINO, S., ed. (1997): *Modular Aspects of Minerals*. European Mineralogical Union, Notes in Mineralogy **1**. Eötvös University Press, Budapest, Hungary.
- MOORE, P.B. (1971): Ericssonite and orthoericssonite. Two new members of the lamprophyllite group, from Långban, Sweden. *Lithos* **4**, 137-145.
- PENG, ZHIZHONG, ZHANG, JIANHONG & SHU, JINFU (1984): The crystal structure of barytolamprophyllite and orthorhombic lamprophyllite. *Kexue Tongbao* **29**, 237-241.
- RASTSVETAeva, R.K., SOKOLOVA, M.N. & GUSEV, A.I. (1990): Refinement of the crystal structure of lamprophyllite. *Mineral. Zh.* **12**(5), 25-28 (in Russ.).
- \_\_\_\_\_, TAMAZYAN, R.A., SOKOLOVA, E.V. & BELAKOVSKII, D.I. (1991): Crystal structures of two modifications of natural Ba, Mn-titanosilicate. *Sov. Phys. Crystallogr.* **36**, 186-189.
- SHELDRIK, G.M. (1997): SHELX-97: Program for the solution and refinement of crystal structures. Siemens Energy and Automation, Madison, Wisconsin.
- SHI NICHENG, MA ZHESHENG, LI GUOWU, YAMNOVA, N.A. & PUSHCHAROVSKY, D.YU. (1998): Structure refinement of monoclinic astrophyllite. *Acta Crystallogr.* **B54**, 109-114.
- SIMONOV, V.I. & BELOV, N.V. (1960): The determination of the structure of seidozerite. *Sov. Phys. Crystallogr.* **4**, 146-157.
- SKSZAT, S.M. & SIMONOV, V.I. (1966): The structure of calcium seidozerite. *Sov. Phys. Crystallogr.* **10**, 505-508.
- SOKOLOVA, E.V., EGOROV-TISMENKO, YU.K. & KHOMYAKOV, A.P. (1988): The crystal structure of sobolevite. *Sov. Phys. Dokl.* **33**, 711-714.

- \_\_\_\_\_, \_\_\_\_\_ & \_\_\_\_\_ (1989): The crystal structure of nacaphite. *Sov. Phys. Dokl.* **34**, 9-11.
- VRÁNA, S., RIEDER, M. & GUNTER, M.E. (1992): Hejtmanite, a manganese-dominant analogue of bafertisite, a new mineral. *Eur. J. Mineral.* **4**, 35-43.
- YAMNOVA, N.A., EGOROV-TISMENKO, YU.K. & PEKOV, I.V. (1998): Crystal structure of perraultite from the coastal region of the Sea of Azov. *Crystallogr. Rep.* **43**, 401-410.
- \_\_\_\_\_, \_\_\_\_\_, ZLYKHENSKAYA, I.V., & KHOMYAKOV A.P. (2000): Refined crystal structure of iron rich triclinic astrophyllite. *Crystallogr. Rep.* **45**(4), 585-590.

*Received March 18, 2001, revised manuscript accepted July 26, 2001.*